Eur. Phys. J. A **25**, s01, 135–138 (2005)
DOI: 10.1140/epjad/i2005-06-037-9

**EPJ A direct**
**electronic only**

# Beta-decay studies near $^{100}$Sn

M. Karny[1,a], L. Batist[2], A. Banu[3], F. Becker[3], A. Blazhev[3,4], K. Burkard[3], W. Brüchle[3], J. Döring[3], T. Faestermann[5], M. Górska[3], H. Grawe[3], Z. Janas[1], A. Jungclaus[6], M. Kavatsyuk[3,7], O. Kavatsyuk[3,7], R. Kirchner[3], M. La Commara[8], S. Mandal[3], C. Mazzocchi[3], K. Miernik[1], I. Mukha[3], S. Muralithar[3,9], C. Plettner[3], A. Płochocki[1], E. Roeckl[3], M. Romoli[8], K. Rykaczewski[10], M. Schädel[3], K. Schmidt[11], R. Schwengner[12], and J. Żylicz[1]

[1] Institute of Experimental Physics, University of Warsaw, Warsaw, Poland
[2] St. Petersburg Nuclear Physics Institute, St. Petersburg, Russia
[3] Gesellschaft für Schwerionenforschung, Darmstadt, Germany
[4] University of Sofia, Sofia, Bulgaria
[5] Technische Universität München, München, Germany
[6] Departamento de Fisica Teórica, Universidad Autonoma de Madrid, Madrid, Spain
[7] Taras Shevchenko Kiev National University, Kiev, Ukraine
[8] Dipartimento Scienze Fisiche, Università "Federico II" and INFN Napoli, Napoli, Italy
[9] Nuclear Science Center, New Delhi, India
[10] Oak Ridge National Laboratory, Oak Ridge, TN, USA
[11] Continental Teves AG & Co., Frankfurt am Main, Germany
[12] Forschungszentrum Rossendorf, Dresden, Germany

Received: 20 December 2004 / Revised version: 14 February 2005 /
Published online: 2 May 2005 – 

**Abstract.** The $\beta$-decay of $^{102}$Sn was studied by using high-resolution germanium detectors as well as a Total Absorption Spectrometer (TAS). A decay scheme has been constructed based on the $\gamma$-$\gamma$ coincidence data. The total experimental Gamow-Teller strength $B_{\rm GT}^{\rm exp}$ of $^{102}$Sn was deduced from the TAS data to be 4.2(9). A search for $\beta$-delayed $\gamma$-rays of $^{100}$Sn decay remained unsuccessful. However, a Gamow-Teller hindrance factor $h = 2.2(3)$, and a cross-section of about 3 nb for the production of $^{100}$Sn in fusion-evaporation reaction between $^{58}$Ni beam and $^{50}$Cr target have been estimated from the data on heavier tin isotopes. The estimated hindrance factor is similar to the values derived for lower shell nuclei.

**PACS.** 21.10.-k Properties of nuclei; nuclear energy levels – 23.40.-s $\beta$ decay; double $\beta$ decay; electron and muon capture – 27.60.+j $90 \leq A \leq 149$

## 1 Introduction

For several years $\beta$-decay studies have tried to answer the question: why two different values for the axial-vector ($g_A$) coupling constant are needed, one for the description of the free neutron decay and another one for $\beta$-decay of atomic nuclei? In the latter case a renormalization of $g_A$ is required in order to get agreement between experimental data and theoretical predictions. Although a final explanation of the problem is the subject of the theoretical work, experiment should yield relevant data for a meaningful comparison. The experimentally derived quantity which can be directly compared to the theoretical predictions is the strength function. In some regions of the chart of nuclei due to the non-occurrence of Fermi-type transitions this can be limited to the Gamow-Teller (GT) strength function. In this case the theoretically derived GT strength is just the squared matrix element of the free $\sigma\tau$ operator acting between the initial ($\Psi_i$) and final ($\Psi_f$) wave functions:

$$B_f^{\rm th} = \langle \Psi_f | \sigma\tau | \Psi_i \rangle^2. \quad (1)$$

$B_f^{\rm th}$ should be compared to the experimental value derived as

$$B_f^{\rm exp} = \frac{6147\ {\rm s}}{(g_A/g_V)^2} \cdot \frac{I_\beta}{f(Q_{\rm EC} - E^*) \cdot T_{1/2}}, \quad (2)$$

where $g_A$ and $g_V$ are the axial-vector and vector coupling constants, respectively, $I_\beta$ the $\beta$-decay intensity to the final level $f$, $Q_{\rm EC}$ the total decay energy available, $f(Q_{\rm EC} - E^*)$ the statistical rate function for the transition to the level at the excitation energy $E^*$, and $T_{1/2}$ the half-life of the decaying nucleus (in seconds).

[a] Conference presenter; e-mail: karny@mimuw.edu.pl

**Table 1.** Hindrance factors derived for light nuclei.

| Shell | $h_{\rm high}$ | Reference |
|---|---|---|
| $p$ | 1.49(3) | [1] |
| $sd$ | 1.67(4) | [2] |
| $pf$ | 1.81(4) | [3] |

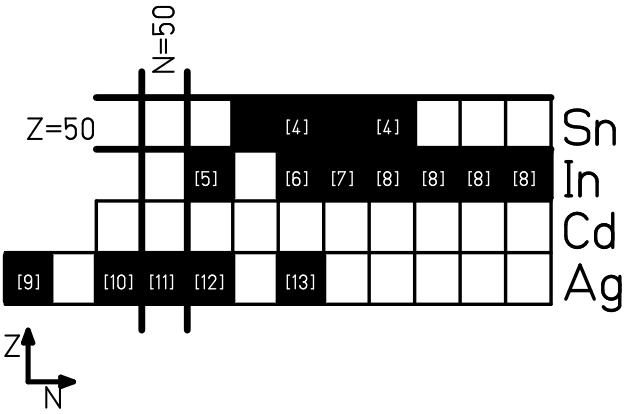


**Fig. 1.** Section of the chart of nuclides near $^{100}$Sn, with full squares representing isotopes studied at the GSI on-line mass separator with focus on the total GT strength determination. Numbers [4,5,6,7,8,9,10,11,12,13] refer to the papers reporting results of the corresponding studies.

The ratio between the summed GT strength from theory and experiment defines a hindrance factor $h$

$$h = \frac{\sum_f B_f^{\rm th}}{\sum_f B_f^{\rm exp}} = \frac{B_{\rm GT}^{\rm th}}{B_{\rm GT}^{\rm exp}}\,. \qquad (3)$$

The hindrance factor defined above can be split into two components $h = h_{\rm low}{\cdot}h_{\rm high}$, with $h_{\rm low}$ being due to the limitation of the shell model calculation used, while $h_{\rm high}$ being associated with higher-order effects. The $h_{\rm low}$ value is assumed to be 1 for a large-space shell model calculations ($0\hbar\omega$), while $h_{\rm high}$ is directly linked to the quenching factor $q$ used to renormalize the axial-vector coupling constant ($h_{\rm high} = 1/q^2$). The hindrance factors derived for lighter nuclei [1,2,3] show a weak mass dependence as presented in table 1.

Beta-decay studies near $^{100}$Sn provide more information on the mass dependence of the hindrance factor. For exotic nuclei around $^{100}$Sn most of the GT strength is expected to be located within the $Q_{\rm EC}$ window enabling observation via $\beta$-decay techniques. Moreover, $\beta$-decay in this region is governed by the pure GT transition of $g_{9/2}$ protons to $g_{7/2}$ neutrons. Figure 1 summarizes the $\beta$-decay studies in the $^{100}$Sn region performed by using the GSI on-line mass separator for determining the total GT strength [4,5,6,7,8,9,10,11,12,13]. In this contribution we present preliminary results of the study of $^{102}$Sn $\beta$-decay performed on the GSI on-line mass separator as well as results of a search for $^{100}$Sn $\beta$-delayed $\gamma$-rays.

## 2 Experimental techniques

The tin isotopes were produced in fusion-evaporation reactions between $^{58}$Ni beam and $^{50}$Cr target. On the basis of HIVAP calculations the beam energies on target were set to maximize the cross-section, *i.e.* 4.6 MeV/$u$ and 5.8 MeV/$u$ for $^{102}$Sn and $^{100}$Sn, respectively. Targets of around 3 mg/cm$^2$ were placed inside a FEBIAD-B2C ion source, which was operated with the addition of $CS_2$ and thus very selectively produced tin nuclei as $SnS^+$ molecular ions [14]. Two complementary experimental set-ups were used for decay spectroscopy of mass-separated samples. Set-up (i) was a high-resolution array consisting of one Cluster, two Clover and 2 smaller volume coaxial detectors for $\gamma$-ray detection ($\epsilon_\gamma = 7.9\%$ for 1.3 MeV $^{60}$Co line) surrounding the Si detectors for $\beta$-particle detection ($\epsilon_\beta = 40\%$). Mass-separated ions were implanted into a mylar tape which was positioned in the center of the set-up (i) and was used to remove the implanted activity after measuring times of 4 s. Set-up (ii) consisted of the Total Absorption Spectrometer (TAS) [15]. In this case mass-separated ions were implanted into the mylar tape and periodically moved into the center of TAS for 4 s of measurement. Set-up (i) allowed us to establish the decay scheme based on $\gamma$-intensity and $\gamma$-$\gamma$ coincidence data, while the TAS yielded information on the $\beta$-feeding to excited states in $^{102}$In, and thus on the GT strength.

## 3 Beta-decay of $^{102}$Sn

Figure 2 shows the $^{102}$Sn decay scheme including two levels (dashed lines) which were added to the decay scheme in order to reproduce the TAS spectrum. The accuracy of the energy of the latter two levels is approximately 30 keV. The level scheme shown in fig. 2 resembles the main structure of that proposed earlier by Stolz *et al.* [16,17] without knowledge of $\gamma$-$\gamma$ coincidences. The main difference is the non-observation of a 53 keV line in our experiment and thus a change in the tentative $^{102}$In ground-state spin assignment from $(7^+)$ to $(6^+)$. This assignment is consistent with the one adopted in in-beam studies [18]. The TAS-based $\beta$-feedings ($I_\beta$) and comparative half-lives ($\log(ft)$) are also shown in fig. 2, yielding the total $B_{\rm GT}^{\rm exp}$ value of 4.2(9) for the decay of $^{102}$Sn. This value, compared to a theoretical calculation performed in a $\pi(p_{1/2}, g_{9/2})^{11}$, $\nu(g_{7/2}, d_{5/2}, d_{3/2}, s_{1/2}, h_{11/2})^3$ model space [19], yields a hindrance factor of 3.7(7). This result agrees qualitatively with the hindrance factors obtained for other nuclei around $^{100}$Sn, *i.e.* $^{97}$Ag: 4.3(6) [11], $^{98}$Ag: 4.6(6) [12], $^{98}$Cd: 3.8(7) [19], $^{100}$In 4.1(9) [5]. Unfortunately, large-space shell model calculation cannot be performed for $^{102}$Sn decay and therefore it is not possible to deduce the $h_{\rm high}$ part of the hindrance factor for this nucleus. Nevertheless the systematics of the $B_{\rm GT}^{\rm exp}$ values and the resulting hindrance factor in the vicinity of $^{100}$Sn will be discussed in sect. 5.

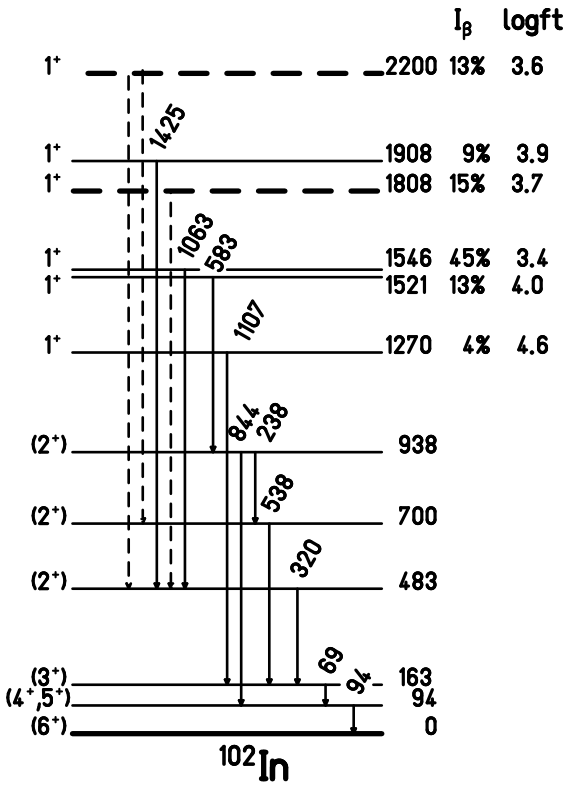


**Fig. 2.** $^{102}$Sn $\beta$-decay scheme. Transitions and levels established in the high-resolution experiment are presented by solid lines. Dashed lines represent levels and $\gamma$-transitions added to the level scheme in order to reproduce the TAS spectrum.

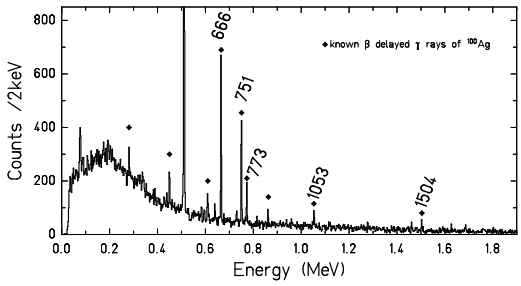


**Fig. 3.** $\beta$-gated $\gamma$ spectrum for $A = 100 + 32$. Lines marked with diamonds belong to the decay of $^{100}$Ag. Some of the strong transitions are marked by their energies in keV.

## 4 Search for $\beta$-delayed $\gamma$-rays of $^{100}$Sn

In the last experiment at the GSI on-line mass separator, which has been decommissioned meanwhile, we spent 69 hours in a search for $\beta$-delayed $\gamma$ rays of $^{100}$Sn. Figure 3 presents a $\beta$-gated $\gamma$ spectrum summed over all detectors. All identified lines (also in $\gamma$-$\gamma$ coincidences) belong to the decay of $^{100}$Ag with a transition intensity above 1% [20].

The sensitivity limit for the search for $\beta$-delayed $\gamma$-rays of $^{100}$Sn was estimated on the basis of the non-observation of a $\gamma$ line between 1 and 2 MeV, that could be assigned to the $^{100}$Sn decay in the $\beta$-gated $\gamma$ spectrum. It was assumed that such a line to be significant should have an

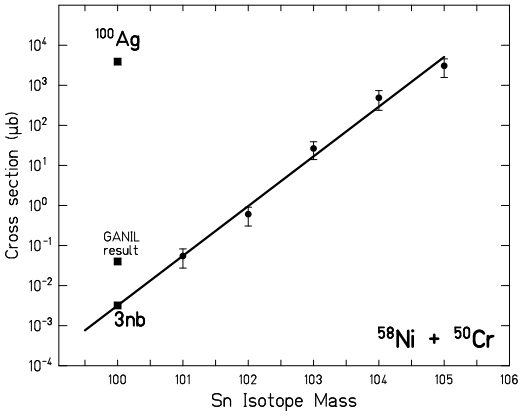


**Fig. 4.** Production cross-section for light tin isotopes, deduced on the basis of the data collected at the GSI on-line mass separator. In the top left corner the cross-section for the production of $^{100}$Ag is shown [21]. The experimental results were obtained at different $^{58}$Ni beam on target energies which range from 3.8 MeV/$u$ for $^{105}$Sn to 5.8 MeV/$u$ for $^{100}$Sn.

area of around $3\sigma$ of the average background in this region and a width of 3 keV, which corresponds to $\approx$ 27 counts. The following input data were used: 5.7% [14,22] for separation efficiency for $SnS^+$ ions of $T_{1/2} = 0.94$ s [23], 45 particle nA for average $^{58}$Ni beam intensity, 3 mg/cm$^2$ for $^{50}$Cr target thickness, 7.5% and 40% for gamma and $\beta$ detection efficiency, respectively, 100% for intensity of the $\gamma$ transition searched for, 4.2 s for the length of the tape cycle (measurement plus transport) and 69 hours for the total measuring time. The resulting estimate of the sensitivity limit is on the level of 10 nb.

The decay data obtained in this work for $^{101}$Sn [24] to $^{105}$Sn yield information on cross-sections for the production of these isotopes in the fusion-evaporation reaction between $^{58}$Ni beam and $^{50}$Cr target. The results are presented in fig. 4. The extrapolated cross-section for the $^{100}$Sn production is about 3 nb. This result is considerably below the previously reported value of 40 nb given in [25] as well as below the achieved sensitivity limit, and explains the non-observation of $^{100}$Sn $\beta$-delayed $\gamma$-rays in this experiment.

## 5 Total Gamow-Teller strength

Figure 5 presents experimental $B_{\rm GT}^{\rm exp}$ results for nuclei around $^{100}$Sn. As can be seen from the data the $B_{\rm GT}^{\rm exp}$ values for neutron-deficient tin and indium isotopes show a linear dependence as a function of the mass number. This feature can be qualitatively interpreted as reflecting the influence of the number of $\pi g_{9/2}$ particles and $\nu g_{7/2}$ holes in the parent and daughter nucleus. By extrapolating the linear $B_{\rm GT}^{\rm exp}$ slope for tin isotopes to $A = 100$, the $B_{\rm GT}$ value of $^{100}$Sn is found to be $\approx 4.7$. This result can be compared to the value of 6.5(1), calculated by using a shell model Monte Carlo method [26]. In this calculation

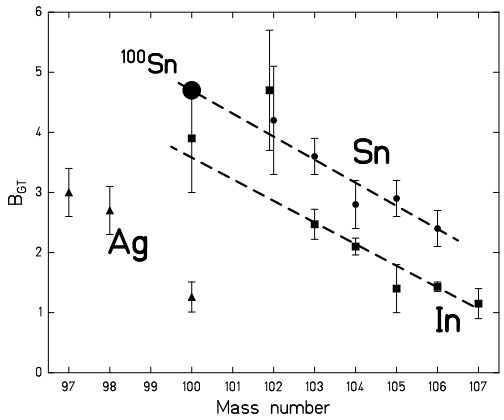


**Fig. 5.** Experimental total $B_{\mathrm{GT}}^{\mathrm{exp}}$ values of isotopes studied at the GSI on-line mass separator. Dashed lines mark the fitted linear dependency for tin and indium isotopes. The large black dot represents the extrapolated $B_{\mathrm{GT}}$ value for $^{100}$Sn.

the $\sigma\tau^+$ operator was renormalized by 1/1.26 [26]. Therefore, in the final comparison $B_{\mathrm{GT}}^{\mathrm{th}} = 6.5(1)\cdot 1.26^2 = 10.3(2)$ should be taken yielding a hindrance factor $h = 2.2$. Since the calculations were performed in the complete $0\hbar\omega$ shell the $h_{\mathrm{low}}$ is 1, yielding $h_{\mathrm{high}} = 2.2$. Although this value is somewhat larger than the hindrance factor for $fp$ shell nuclei (see table 1), uncertainty of about 15% makes the two values comparable. Similar hindrance factors for $fp$ shell nuclei and $^{100}$Sn suggest a flat dependence of the quenching factor for masses of $A = 100$ and higher.

The extrapolated $B_{\mathrm{GT}}$ value can also serve as a basis for the estimate of the position of the only $1^+$ state expected to be fed in the $\beta$-decay of $^{100}$Sn. With a $Q_{\mathrm{EC}}$ value of 7.39(66) [27] and a half-life $T_{1/2} = 0.94^{+0.54}_{-0.27}$ s [23] the $B_{\mathrm{GT}}$ value of 4.7 corresponds to a 100% $\beta$-feeding to a $^{100}$In state at an excitation energy of $\approx 2.3$ MeV.

## 6 Summary

With the use of molecular $SnS^+$ beams at the GSI on-line mass separator the $\beta$-decay of $^{102-105}$Sn has been studied. In this contribution we presented in particular $\beta$-decay studies of $^{102}$Sn. They include high-resolution $\gamma$-$\gamma$ coincidence data, allowing us to build the decay scheme of $^{102}$Sn as well as information on the GT strength distribution from a TAS measurement. Although $\beta$-delayed $\gamma$-rays from $^{100}$Sn have not been observed, the $B_{\mathrm{GT}}^{\mathrm{exp}}$ systematic allowed us to estimate the expected hindrance factor for $^{100}$Sn decay to be $h = 2.2$, in agreement, within the respective uncertainties, with the hindrance factor observed for the lower $fp$ shell.

The authors would like to thank W. Hüller for his contributions to the development and operation of the GSI on-line mass separator. This work was supported in part by the Polish Committee for Scientific Research funds of 2004, under Contract No. 2P03B 035 23, and the European Community RDT Project TARGISOL under Contract No. HPRI-CT-2001-50033.

## References

1. W.T. Chou, E.K. Warburton, B.A. Brown, Phys. Rev. C **47**, 163 (1993).
2. B.H. Wildenthal, M.S. Curtin, B.A. Brown, Phys. Rev. C **28**, 1343 (1983).
3. G. Martinez-Pinedo, A. Poves, E. Caurier, A.P. Zuker, Phys. Rev. C **53**, R2602 (1996).
4. M. Kavatsyuk *et al.*, these proceedings.
5. C. Plettner *et al.*, Phys. Rev. C **66**, 044319 (2002).
6. M. Gierlik *et al.*, Nucl. Phys. A **724**, 313 (2003).
7. M. Karny *et al.*, Nucl. Phys. A **640**, 3 (1998).
8. M. Karny *et al.*, Nucl. Phys. A **690**, 367 (2001).
9. M. La Commara *et al.*, Nucl. Phys. A **708**, 161 (2002).
10. L. Batist *et al.*, Nucl. Phys. A **720**, 245 (2003).
11. Z. Hu *et al.*, Phys. Rev. C **60**, 024315 (1999).
12. Z. Hu *et al.*, Phys. Rev. C **62**, 064315 (2000).
13. L. Batist *et al.*, Z. Phys. A **351**, 149 (1995).
14. R. Kirchner, Nucl. Instrum. Methods Phys. Res. B **204**, 179 (2003).
15. M. Karny *et al.*, Nucl. Instrum. Methods Phys. Res. B **126**, 411 (1997).
16. A. Stolz, PhD Thesis, Universität München, 2001.
17. A. Stolz *et al.*, AIP Conf. Proc. **638**, 259 (2002).
18. D. Sohler *et al.*, Nucl. Phys. A **708**, 181 (2002).
19. B.A. Brown, K. Rykaczewski, Phys. Rev. C **50**, R2270 (1994).
20. B. Singh, Nucl. Data Sheets **81**, 1 (1997).
21. R. Schubart *et al.*, Z. Phys. A **352**, 373 (1995).
22. R. Kirchner, private communication.
23. R. Schneider, PhD Thesis, Universität München, 1996.
24. O. Kavatsyuk *et al.*, submitted to Eur. Phys. J. A.
25. M. Chartier *et al.*, Phys. Rev. Lett. **77**, 2400 (1996).
26. D.J. Dean *et al.*, Phys. Lett. B **367**, 17 (1996).
27. G. Audi, A.H. Wapstra, C. Thibault, Nucl. Phys. A **729**, 337 (2003).